行政院國家科學委員會專題研究計畫　成果報告

系統封裝基板之關鍵技術研究

計畫類別：個別型計畫
計畫編號：NSC93-2216-E-009-023-
執行期間：93 年 08 月 01 日至 94 年 07 月 31 日
執行單位：國立交通大學電子工程學系暨電子研究所

計畫主持人：邱碧秀

報告類型：精簡報告
報告附件：出席國際會議研究心得報告及發表論文
處理方式：本計畫可公開查詢

中　華　民　國 94 年 9 月 2 日

Abstract

This study focuses on the processing and reliability of metal-insulator-metal (MIM) capacitors which may be used as embedded capacitors in the integral substrate for system in package (SiP). It was originally proposed as a two-year research project. However, the project was only granted for one year. Hence, some of the research items proposed in the original proposal were not carried out due to time and budget deficiency. In this study, MIM capacitors with PECVD oxide and nitride were treated with N_2O and SiH_4/NH_3 plasma, respectively, after deposition of the dielectric layer. No apparent change in film microstructure is observed after plasma treatment. Plasma post-treatment is effective in eliminating the electrical hysteresis shift of the nitride capacitors. The time dependent dielectric breakdown testing indicates a decrease in both the leakage current and the lifetime of the MIM capacitors treated with plasma. Possible dielectric degradation mechanism is explored. Besides, the dielectric breakdown field is one of the important concerns for device reliability. The breakdown of dielectric is originated at a fatal flaw that grows to cause failure and can be explained by the weakest-link theory. The Weibull distribution function, which is based on the weakest-link theory, is employed to analyze the effect of the electrode area as well as the plasma treatment on the breakdown of the MIM capacitors.

中文摘要

本研究的重點是可作為系統封裝技術中的整合式基板內埋式電容用的金屬-絕緣層-金屬(MIM)架構的電容。本計畫原規劃為兩年期計畫，但只核准一年，所以原計畫書中的某些工作項目由於時間及經費的限制，沒有執行。

本研究是針對利用 PECVD 鍍覆氧化矽和氮化矽絕緣層來完成 MIM 架構的電容，而在鍍覆絕緣層後，分別針對氧化矽及氮化矽薄膜，利用 N_2O 和 SiH_4/NH_3 作電漿處理。電漿處理可以降低氮化矽薄膜的電滯位移現象。電漿處理後雖會降低漏電流，但卻會導致電容使用壽命的縮短，本研究亦針對可能的機制作討論。

此外，介電崩潰電場也是元件可靠度很重要的課題。本研究發現絕緣層崩潰可以利用 weakest-theory 來解釋。而 Weibull 分佈函數是利用 weakest-theory 為理論基礎，故本研究將採用 Weibull 分佈函數來分析電極面積與電漿處理對於電容的可靠度的影響。

Keywords: Capacitor electrical hysteresis, plasma treatment, reliability, nitride, Weibull distribution, weakest-link theory, dielectric breakdown, PECVD.

Introduction

Integration of precision metal-insulator-metal (MIM) capacitors into substrate has been a key building block for integral substrate for system-in-package (SiP). Silicon-on-silicon packaging has the advantage of perfect match in thermal expansion. Hence, Si substrate is used in this study, and thin film technology is employ to prepare the embedded capacitor. Plasma enhanced chemical vapor deposition (PECVD) has the advantage of depositing insulators in a clean processing vicinity at very low temperatures. The low temperature processing eliminates the segregation or redistribution of the dopants commonly occurred in conventional high temperature processes.

Metal-insulator-metal (MIM) and metal-nitride-semiconductor (MNS) capacitors with PECVD nitride exhibit trap-induced dispersive behavior and electrical hysteresis, which lead to degradation in capacitor linearity at low frequencies, limiting the accuracy in precision analog circuits [1, 2]. The dominant defect responsible for charge trapping in silicon nitride was suggested to be silicon dangling bonds, which originate from a deficiency in nitrogen. Various methods, such as: use of a PECVD oxide-nitride-oxide (ONO) stacks and/or appropriate SiH_4/NH_3 plasma pre-treatment of silicon substrate before the nitride deposition to make the nitrogen to silicon ratio higher at the interfacial region have been employed to eliminate the dispersive behavior and electrical hysteresis [1, 2]. However, very few work reported on the effect of the plasma post-treatment on the electrical behaviors of the dielectric films.

In this study, MIM capacitors with PECVD oxide and nitride were treated with N_2O and SiH_4/NH_3 plasma, respectively, after deposition of the dielectric layer. The effects of plasma post-treatment on the microstructure, the electrical behaviors, and the reliability of the dielectric thin films are investigated. The effects of electrode area and plasma treatment on the breakdown strength of the dielectric are investigated using Weibull distribution.

Experimental Procedures

Four inch diameter p-type (100) Si wafers with nominal resistivity of 1 to 10 Ω-cm were used as substrate. After standard RCA cleaning, a 100nm SiO_2 film was grown on the Si substrate. A 100nm Al films were deposited by thermal evaporation coater onto the SiO_2/Si substrate to serve as the bottom electrode. Two dielectrics, SiO_2 and SiN_x, were prepared in this study. The amorphous SiO_2 films, deposited by the decomposition of tetraethyl orthosilicate, with 100nm in thickness were deposited onto the bottom electrode with PECVD. The silicon nitride films, with a thickness of 50nm, were deposited with the same PECVD system using a $SiH_4/NH_3/N_2$ mixture. The flow rates of SiH_4, NH_3 and N_2 were fixed at 20, 80, and 510 sccm, respectively. The SiO_2 films were treated with N_2O plasma (with a flow rate of 200 sccm) for 30min, while the SiN_x films were treated with SiH_4/NH_3 plasma (the flow rate are 20 and 700 sccm) for 30min. Aluminum films (150nm) were then deposited as the top electrodes.

Field emission scanning electron microscope (FESEM) (S-4000 Hitachi, Japan) was employed to observe the surface morphology and microstructure of the films. Atomic force microscope (AFM) was employed to measure the surface morphology and roughness. Auger electron microscope (AES) was employed to analyze elemental depth profiles. A C-V analyzer (model 590, Keithley Instruments Inc., U.S.A.) and a semiconductor parameter analyzer (HP4155B, Hewlett Packard Co., U.S.A.) were employed to measure the capacitance and the leakage current, respectively. The time to dielectric failure was defined when the current density exceeded $0.5A/cm^2$.

The electrode areas of capacitors in this study are: $0.237mm^2$ (radius r = 275 μm), $0.159mm^2$ (r=225μm), and $0.096mm^2$ (r=175μm). The current-voltage (I-V) measurement was carried out with a semiconductor parameter analyzer (HP4155B, Hewlett Packard Co., U.S.A.) at 25°C and 150°C. The breakdown field is defined when the leakage current density exceeds $4.21 \times 10^{-3} A/mm^2$.

Results and Discussion

As summarized in Table 1, the capacitance densities increase from 1.02 to $1.21fF/\mu m^2$ for nitride capacitors and from 0.39 to $0.46fF/\mu m^2$ for oxide capacitors after plasma treatment. The voltage dependence of capacitance (C), as exhibited in Fig. 1, can be approximated by:

$$C=C_o(1+AV+BV^2) \quad (1)$$

Where C_o is the capacitance at zero volts, A and B are the linear and quadratic coefficients of the capacitance, respectively. Also listed in Table 1 are the voltage coefficients of capacitance (VCC) from previous works for comparison [1, 3, 4]. The sensitivity of capacitance to bias voltage, i.e., VCC, is one of the important parameters for precision analog design. The specifications demanded by analog designers in the VCC of high precision capacitors are A<50ppm/V and B<10ppm/V [1]. There are many factors which would affect the VCC of the capacitors, including: dielectric composition, processing conditions, dielectric thickness, frequency of measurement, voltage range of measurements and so on.

Plasma treatment eliminates the electrical hysteresis shift of the nitride capacitors. There is a 0.91V shift in the C-V plot for nitride capacitor without plasma treatment (Fig. 2(a)), while no hysteresis shift is observed for plasma treated ones (Fig. 2(b)). For oxide capacitors, no hysteresis shift in the C-V curve is observed. The hystersis phenomenon is believed to be induced by the bulk silicon nitride traps such as: silicon dangling bonds near the nitride/electrode interface [2].

The current density (J) versus electrical field (E) curves, shown in Fig. 3, indicates a decrease of the leakage current density after plasma treatment. The leakage current of the oxide capacitors drops from $1.90 \times 10^{-7} A/cm^2$ of the as-deposited films to $2.91 \times 10^{-10} A/cm^2$ of the plasma-treated ones at 1.0MV/cm. It is argued that the incorporation of nitrogen into the oxide films after N_2O plasma treatment reduces strained Si-O bonds and silicon

dangling bonds, thus, consequently, reduces interface defects and improves the J-E characteristics of the SiO_2 films [5]. The leakage current of the nitride capacitors at 1.0MV/cm reduces from $1.79 \times 10^{-9}A/cm^2$ (as-deposited) to $8.99 \times 10^{-10}A/cm^2$ (plasma-treated). Both the band gap and the barrier heights at the metal-insulator interfaces of the nitride films increase with the increase of the N content [6]. Auger depth profiling results suggest that the nitrogen concentration increases after plasma treatment. Hence, the decrease of the leakage current is attributed to the reduction of the trap densities, the raise of the energy band gap and/or the increase of the barrier height. Fig. 4 exhibits the time (t) dependence of the current density (J) of nitride capacitors at various stress fields. The J-t curves of specimens without plasma treatment show an initial increase of the current density with time followed by a decrease of J with t before the breakdown of the dielectric, while the current density of the plasma-treated samples increases slightly before the breakdown of the dielectric. Besides, although the current density of the plasma-treated capacitors is smaller, the time to dielectric breakdown (TTDB) is shorter.

The breakdown of dielectric is thought to originate at a fatal flaw that grows with time. In the same way that a weak link threatens the integrity of a chain, so too defects of critical size will cause failure in electronic components. The weakest-link theory gives the cumulative probability F(E) that breakdown occurs below electric field E for Weibull distribution as [7] :

$$F(E) = 1 - \exp(-E/E_0)^m \quad (2)$$

$$1 - F(E) = \exp(-E/E_0)^m \quad (3)$$

$$\ln(-\ln(1-F(E))) = m \times \ln(E) - m \times \ln(E_0) \quad (4)$$

where E_0 is the characteristic breakdown field which is the field when 63.2% of capacitors breaks down, and m is called the slope parameter. Since m is the slope of the $\ln[-\ln(1-F(E))]$ versus $\ln(E)$ plot.

Figure 5 is the cumulative breakdown fraction at an electric field E versus E plots as a function of electrode area measured at 25°C and 150°C of silicon dioxide MIM capacitors without plasma treatment, while Fig. 6 is that of oxide MIM capacitors with plasma treatment. Figs 7 and 8 are the breakdown fraction versus E of nitride MIM capacitor. The values of m and E_0 are then evaluated from Figs. 5, 6, 7, and 8 and summarized in Tables 2 and 3. Also listed in Tables 2 and 3 are the parameters χ^2 and R^2 for goodness of fitting. The parameter χ^2 measures the amount of disagreement between the observed data and the expected data, while the parameter R^2 is the coefficient of determination in the regression [8]. As shown in Tables 2 and 3, the χ^2 values are smaller than 0.00478 and the R^2 values are close to 1 (larger than 0.952). This suggests that the Weibull distribution function fits the experimental data.

Conclusions

In this study, SiH_4/NH_3 and N_2O plasmas are used to bombard nitride and oxide films

of MIM capacitors, respectively. The SiH_4/NH_3 plasma treatment eliminates the electrical hysteresis shift of the nitride MIM capacitors. The leakage current density of both the oxide and nitride capacitors decreases after plasma treatment. For oxide capacitors, the incorporation of nitrogen into oxide films reduces interface defects and, hence, the leakage current. For nitride capacitors, there are several possibilities for the decreased leakage current after plasma treatment, such as: the reduction of the trap densities, the raised of the energy bond gap and/or the increase of the barrier height [9].

Weibull distribution function is employed to analyze the electrode area effect on the breakdown strength of the oxide and nitride MIM capacitors. The Weibull distribution function fits the experimental data well with χ^2 values of smaller than 0.00478 and the R^2 values of larger than 0.952. This suggests that the breakdown of the dielectric can be explained with the weakest-link theory, since Weibull distribution function is based on the weakest-link theory [10].

References

[1] S. VAN HUYLENBROECK, S. DECOUTERE, R. VENEGAS, S. JENEI, and G. WINDERICKX, IEEE Electron Device Lett. 23 (2002) 191.

[2] W.S LAU, Jpn. J. Appl. Phys. 29 (1990) L690.

[3] A. KAR-ROY, C. HU, M. RACANELLI, C. A. COMPTON, P. KEMPF, G. JOLLY, P. N. SHERMAN, J. ZHENG, Z. ZHANG, and A. YIN, in Proceedings of the 2nd IEEE International Interconnect Technology Conference, San Francisco, USA, May 1999 (IEEE, New York, USA, 1999) p. 245.

[4] J. A. BABCOCK, S. G. BALSTER, A. PINTO, C. DIRNECKER, P. STEINMANN, R. JUMPERTZ, and B. El-KAREH, IEEE Electron Device Lett. 22 (2001) 230.

[5] S. R. KALURI and D. W. HESS, J. Electromchem. Soc. 145 (1998) 662.

[6] M. H. W. M. VAN DELDEN and P. J. VAN DER WEL, in Proceedings of the 41st International Reliability Physics Symp. Dallas, USA, March 2003 (IEEE, New York, USA, 2003) p. 293.

[7] M. Ohring, Reliability and failure of electronic materials devices, San Diego California: Academic Press Ltd; 1998, p. 208-11, 310-28.

[8] LJ. Kitchens, Exploring statistics: a modern introduction to data analysis and inference, 2nd ed. Belmont California: Duxbury Press; 1998, p. 641-5, 737-41.

[9] C. C. Ho, B. S. Chiou, J. Mater. Sci. Mater. Electron., (submitted)

[10] C. C. Ho, B. S. Chiou, Micro. Rel., (submitted)

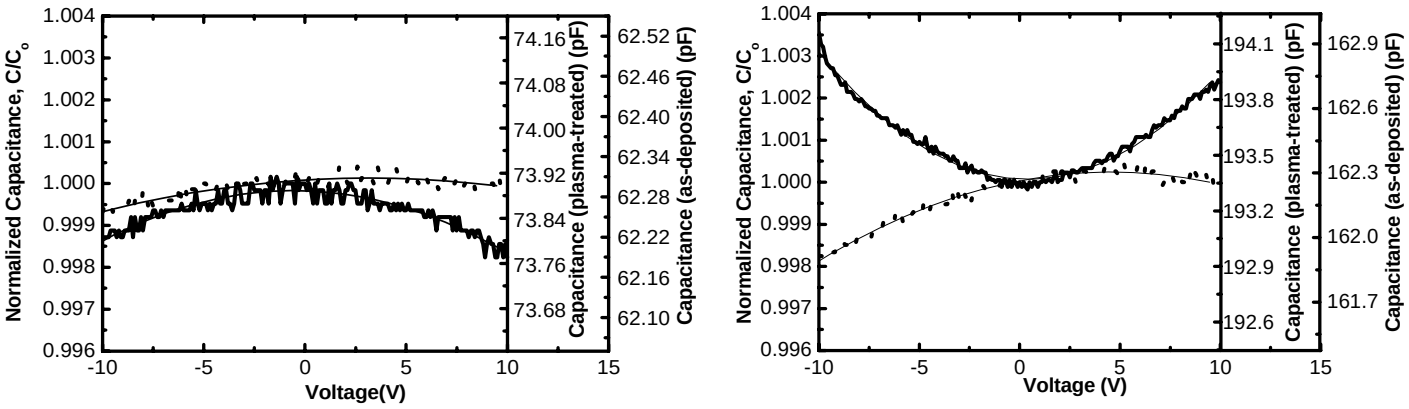

[11] **(a)** **(b)**

Fig. 1 Capacitance (C) as a function of the dc voltage of (a) oxide and (b) nitride MIM capacitors with (●●●●●) and without (▬) plasma treatment. The curves exhibit quadratic behavior in the voltage coefficient of capacitance (VCC). C_o is the capacitance value measured at 0 volt.

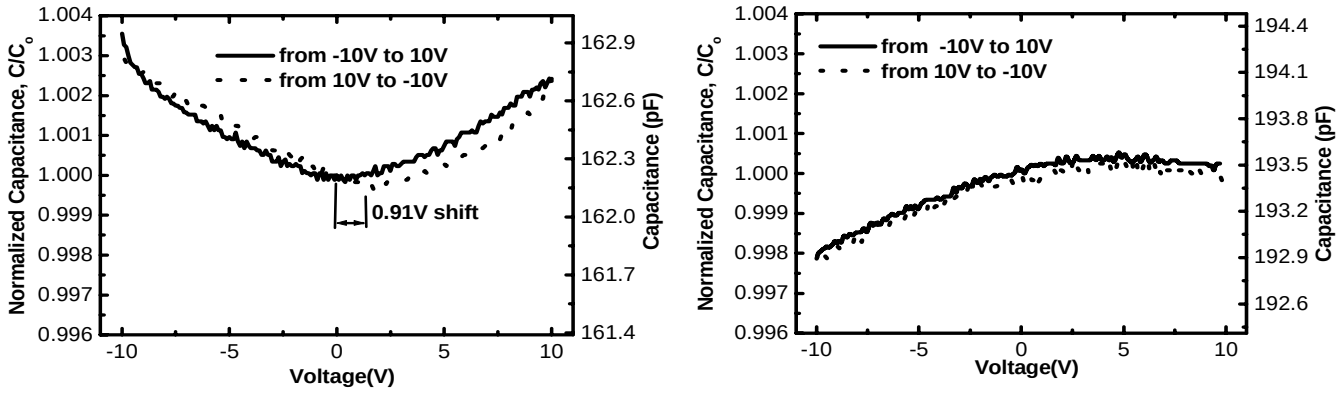

(a) **(b)**

Fig. 2 Capacitance (C) as a function of the dc voltage of nitride MIM capacitors without and (b) with plasma treatment. C_o is the capacitance value measured at 0 volt from –10V to 10V.

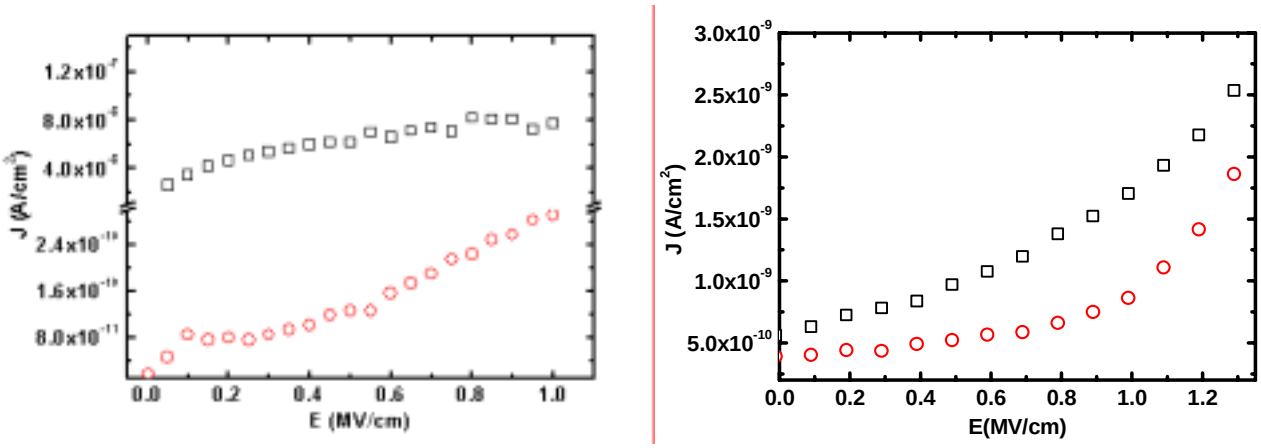

(a) **(b)**

Fig. 3 Current density (J) versus electrical field (E) of as-deposited (□) and plasma-treated (○) (a) SiO_2 and (b) SiN_x MIM capacitors measured at room temperature.

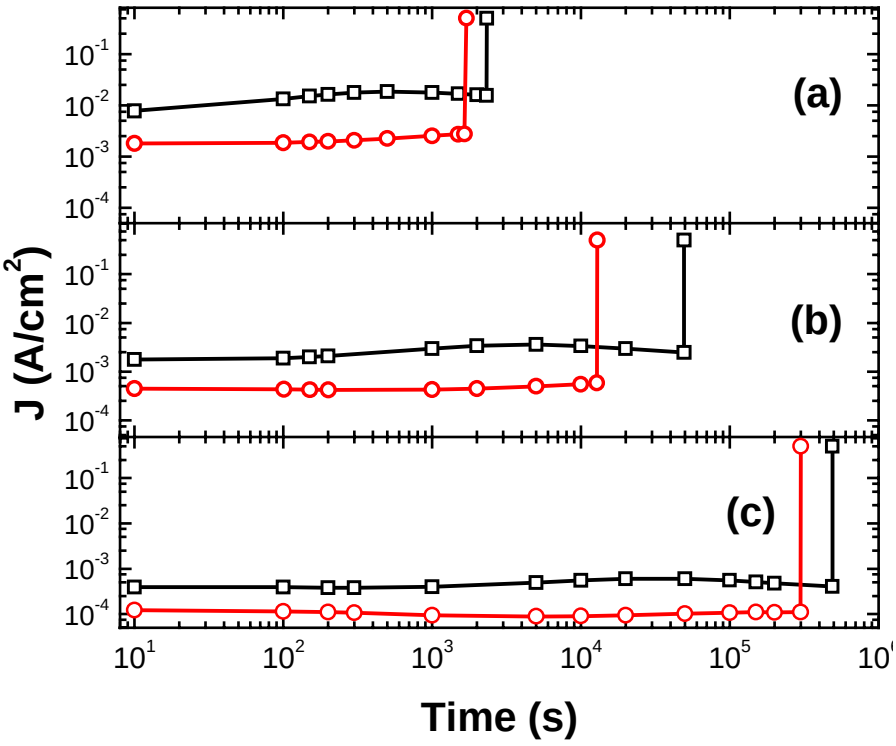

Fig. 4 Time dependence of the current density of nitride capacitors with (○) and without (□) plasma treatment at (a) 6.0MV/cm, (b) 5.5MV/cm, and (c) 5.0MV/cm.

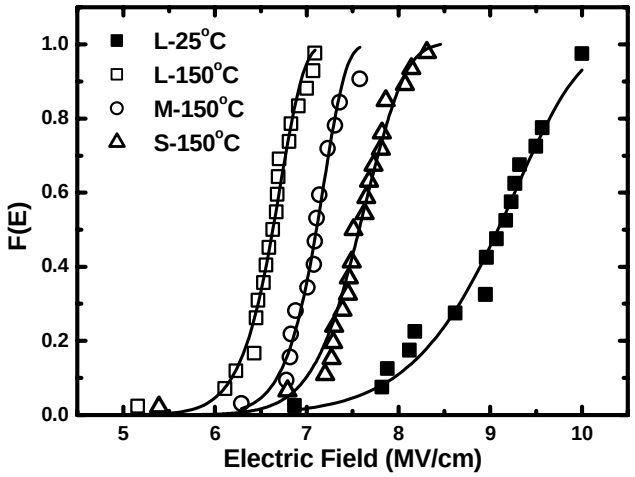

Fig. 5 The cumulative capacitor breakdown fraction F(E) as a function of electric field E of as-deposited SiO_2 MIM capacitors with various electrode area. Lines are the curves fitted with Weibull distribution function.

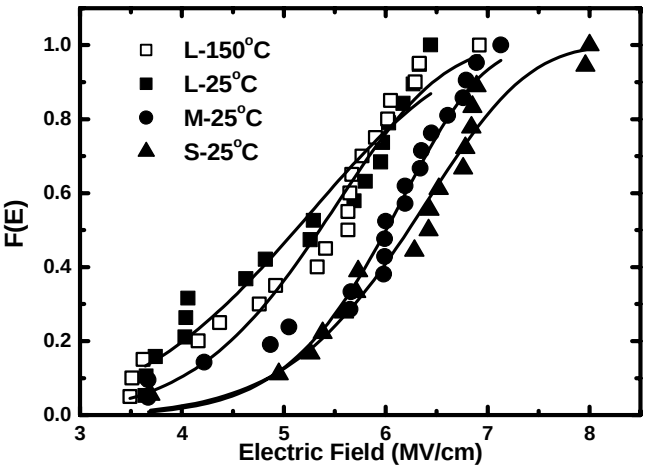

Fig. 6 The cumulative capacitor breakdown fraction F(E) as a function of electric field E of plasma-treated SiO_2 MIM capacitors with various electrode area. Lines are the curves fitted with Weibull distribution function.

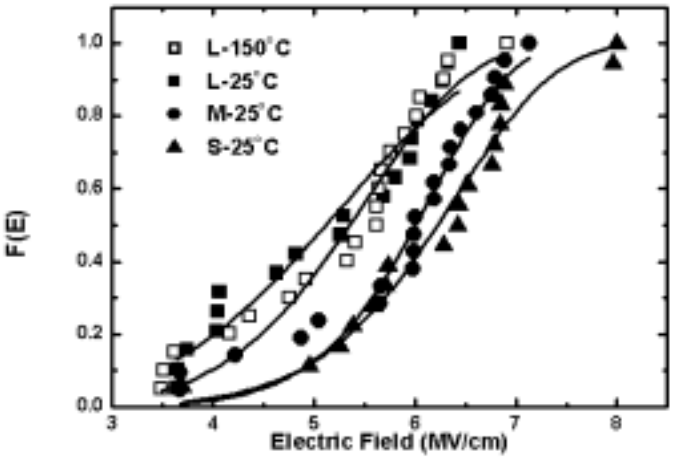

Fig. 7 The cumulative capacitor breakdown fraction F(E) as a function of electric field E of as-deposited SiN_x MIM capacitors with various electrode area. Lines are the curves fitted with Weibull distribution function.

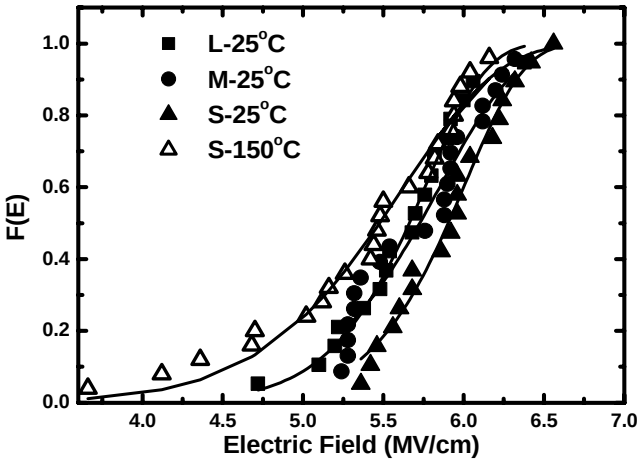

Fig. 8 The cumulative capacitor breakdown fraction F(E) as a function of electric field E of plasma-treated SiN_x MIM capacitors with various electrode area. Lines are the curves fitted with Weibull distribution function.

Table 1 Capacitance density and voltage coefficient of capacitance, A and B*, of several nitride and oxide MIM capacitors at 100kHz.

Capacitance density (fF/μm^2)	Voltage range of measurement	Dielectric thickness (nm)	A(ppm/V)	B(ppm/V^2)	Note
1.02 (as-deposited nitride)	10V to -10V	50	-22.1	27.9	This work
1.21 (plasma-treated nitride)			91.5	-9.8	
0.39 (as-deposited oxide)	10V to –10V	100	-14.6	-13.4	This work
0.46 (plasma-treated oxide)			29.1	-4.6	
1.1 (nitride)	5V to -5V	60	25.5	9.3	Ref.1
1.2~1.35 (nitride)	5V to -5V	50	-21~-14	5.5~8	Ref.3
2.0 (nitride)	6V to -6V	30	-153	62.3	Ref.4

* $C=C_o(1+AV+BV^2)$. C_o and C are the capacitances at 0 and V volts, respectively.

Table 2 Weibull slope parameter m* and characteristic electric field E_0* for the cumulative breakdown of SiO_2 MIM capacitors with and without plasma treatment.

	Without plasma treatment			
A^{ζ} / $T(^oC)$ / parameter	0.237	0.159	0.096	0.237
	150	150	150	25
m	26.86	30.22	26.21	14.04
E_0	6.76	7.14	7.69	9.34
$\chi^{2\,\#}$	0.00170	0.00188	0.00141	0.00185
$R^{2\,\#}$	0.9812	0.9781	0.9740	0.9776
	With plasma treatment			
A^{ζ} / $T(^oC)$ / parameter	0.237	0.159	0.096	0.237
	25	25	25	150
m	4.66	8.88	7.50	6.35
E_0	5.55	6.25	6.53	5.68
$\chi^{2\,\#}$	0.00478	0.00350	0.00301	0.00403
$R^{2\,\#}$	0.943	0.963	0.968	0.956

Table 3 Weibull slope parameter m* and characteristic electric field E_0* for the cumulative breakdown of SiN_x MIM capacitors with and without plasma treatment.

	Without plasma treatment			
A^{ζ} / $T(^oC)$ / parameter	0.237	0.159	0.096	0.096
	150	150	150	25
m	11.47	11.58	10.38	9.51
E_0	3.55	4.17	4.44	4.52
$\chi^{2\,\#}$	0.00484	0.00030	0.00440	0.00366
$R^{2\,\#}$	0.956	0.974	0.967	0.963
	With plasma treatment			
A^{ζ} / $T(^oC)$ / parameter	0.237	0.159	0.096	0.096
	25	25	25	150
m	16.26	13.03	17.27	10.31
E_0	5.81	5.91	6.02	5.68
$\chi^{2\,\#}$	0.00064	0.00368	0.00159	0.00183
$R^{2\,\#}$	0.992	0.952	0.983	0.980

* Derived from data measured at 25°C and/or 150°C.

ζ Electrode area (mm^2).

Statistic parameters for goodness of fitting [8].

計畫成果自評部分

本計畫原規劃為兩年期計畫，但只核准一年，所以原計畫書中的某些工作項目由於時間及經費的限制，沒有執行。有執行的工作項目的部分研究成果已整理兩篇文章投稿國際期刊，論文名稱與投稿期刊分別為 Effect of Plasma Treatment on the Microstructure and Electrical Properties of Thin Film MIM Capacitors (Journal of Materials Science: Materials in Electronics)和 Effect of Size and Plasma Treatment and the Application of Weibull Distribution on the Breakdown of Thin Film Capacitors (Microelectronics Reliability)，第三篇正在撰寫中。